Kinome Inhibition States and Multiomics Data Enable Prediction of Cell Viability in Diverse Cancer Types

Matthew E. Berginski*, Chinmaya U. Joisa*, Brian T. Golitz, Shawn M. Gomez

Departments of Pharmacology and Biomedical Engineering at the University of North Carolina at Chapel Hill
Corresponding Author: Shawn Gomez (smgomez@unc.edu)

Abstract

Protein kinases play a vital role in a wide range of cellular processes and compounds that inhibit kinase activity have emerged as a primary focus for targeted therapy development in cancer. This has inspired work that characterizes the spectrum of kinases targeted by specific inhibitors and the inclusion of these inhibitors in large-scale cell viability screening efforts. Previous work with smaller datasets have used baseline profiling of cell lines and limited kinome profiling data to attempt to predict small molecule effects on cell viability, but these efforts did not use multi-dose kinase profiles and achieved low accuracy with very limited external validation. This work focuses on two primary data types, kinase inhibitor profiles and gene expression, to predict the results of cell viability screening. We describe the process by which we combined these data sets, examined their properties in relation to cell viability and finally developed a set of computational models that achieve reasonable prediction accuracy (R^2 of 0.78 and RMSE of 0.154). Using these models, we identified a set of kinases, several of which are understudied, that are strongly influential in the cell viability prediction models. In addition, we also tested to see if a wider range of multiomics data sets could improve the model results. Finally, we validated a small subset of the model predictions in several triple-negative and HER2 positive breast cancer cell lines demonstrating that the model performs well with compounds and cell lines that were not included in the training data set. Overall, this result demonstrates that generic knowledge of the kinome is predictive of very specific cell phenotypes, and has the potential to be integrated into targeted therapy development pipelines.

Introduction

While chemotherapy remains a mainstay in cancer treatment, the use of targeted therapies clearly holds significant promise, with their use leading to improved outcomes in a variety of cancers (Falzone et al., 2018; Keefe and Bateman, 2019). Examples include the use of imatinib (Gleevec) for chronic myelogenous leukemia, crizotinib and other anaplastic lymphoma kinase (ALK) inhibitors for non-small-cell lung cancers, and trastuzumab and lapatinib for ERBB2/HER2 amplified breast cancers (Deininger et al., 2009; Geyer et al., 2006; O'Brien et al., 2003; Slamon et al., 2001; Solomon et al., 2014; Yuan et al., 2019). Together with the potential to reduce toxicity and associated side effects, the development of targeted therapies has gained increasing momentum over the last two decades (Seebacher et al., 2019; Zhong et al., 2021).

Since the development of imatinib, protein kinases have emerged as a primary focus for targeted therapy development (Attwood et al., 2021; Bhullar et al., 2018; Cohen et al., 2021; Pottier et al., 2020). Kinases are a ~500-member enzyme family that catalyzes the transfer of phosphate groups from ATP to specific substrates. Integrated into a complex network of interactions defined as the kinome, kinases regulate information transfer across a myriad of cellular processes including growth, proliferation, differentiation, motility, and apoptosis (Shapiro, 2020). Linked to its role in this wide array of functions, dysregulation of one or more members of the kinome is directly implicated in numerous pathologies, especially cancer (Lahiry et al., 2010). Modulation of kinase activity through targeted inhibition has been the primary therapeutic approach to date and as of 2021, over 85 kinase inhibitors have been clinically approved worldwide, though only targeting 42 kinases from the 21 kinase families(Laufer and Bajorath, 2022), highlighting the opportunity for further advancement of this druggable target.

Recent work characterizing kinome behavior in response to targeted kinase inhibitor therapies has established that the kinome is a highly dynamic system, with significant ramifications in our understanding of drug resistance, adaptive reprogramming and the broader design of effective therapies (Collins et al., 2018; Duncan

et al., 2012; Frejno et al., 2017; Golkowski et al., 2020; Yesilkanal et al., 2021; Zawistowski et al., 2017). Underlying these investigations of kinome dynamics are the advancement of proteomic approaches that enable the characterization of protein kinome behavior in response to perturbation en masse, allowing characterization of changes not just to the kinase to which the inhibitor was designed, but also across the entire kinome (Bantscheff et al., 2007; Plowright, 2019). However, while providing transformative insight into how these targeted therapies interact with and modify cellular systems, our understanding of kinome changes and the resulting downstream cellular changes is still lacking.

Given the potential of targeted therapies and the potential to quantitatively assess their effect on the protein kinome, in this work we sought to establish a predictive framework that links the behavior of the kinome as defined by “kinase inhibition states" with a downstream phenotype - in this instance, cell viability. Enabling this effort is recent work by Klaeger et al., who conducted a comprehensive investigation using a proteomic kinobead approach, establishing a target landscape for 229 kinase inhibitors across a wide range of compound concentrations (Klaeger et al., 2017). In addition, we utilized the extensive data available via the Broad Institute’s Cancer Cell Line Encyclopedia (CCLE)(Ghandi et al., 2019), including the PRISM (Profiling Relative Inhibition Simultaneously in Mixtures) highly multiplexed cell viability assay, along with accompanying multi-omics data (gene expression, copy number variation, proteomics and gene essentiality) from the Cancer Dependency Map. These data consist of cell viability measurements for 499 cell lines across 1448 drugs, transcriptomic profiles for 1389 cell lines, whole proteomic profiles for 375 cell lines, whole genome copy number variation for 1750 cell lines and CRISPR-KO genetic dependency scores for 1054 cell lines. While predictive models for drug-induced cell viability have been built using various strategies (Corsello et al., 2020; Daemen et al., 2013; J. Lu et al., 2021; Lu J. et al., 2021), most have focused on using baseline and drug-perturbed transcriptomic data to make predictions on the sensitivity of cancer cell lines to drugs. Drug-target interaction data like kinome profiles are relatively underutilized in these approaches, but have been shown to have predictive power in smaller datasets(Vidović et al., 2014).

Here, we describe a framework that integrates kinome profiling data with general multi-omics, and build tree-based regression models to predict cell viability for 480 cancer cell lines across 230 kinase inhibitors with high accuracy (R^2 = 0.79). Integrating nearly half a million data points, we find that kinome inhibition profiles have by far the greatest predictive power of any single data set. While not highly predictive on its own, baseline transcriptomic data does significantly enhance prediction accuracy, “tuning” the model to individual cell lines. Remarkably, adding in other multi-omics data does not significantly increase the quality of predictions. As the model enables prediction of complete dose-response curves, we experimentally validate predictions for over two dozen compounds on two breast cancer cell lines and find strong agreement for most compounds tested. These results suggest that the link between kinotype and phenotype is significant, with sufficient power to enable the prediction of cell viability and likely other cellular phenotypes as well. Along with integration of transcriptional data, these predictive models can greatly enhance our understanding of adaptive kinome reprogramming and drug resistance while facilitating the development of future targeted therapy regimes.

Results

This work is divided into three parts. We start by describing how we processed and organized the data sets used to build predictive models of cell viability related to a set of kinase inhibitors. Next, we describe the methods we used to select which features and data sets to include in these models and apply a set of modeling methods to the organized data. Finally, we make a set of cell viability predictions and then experimentally test these predictions in a panel of breast cancer cell lines.

Linking Kinome Inhibitor States with Cancer Cell Viability

There are two primary data sources that we needed to process and combine in order to link kinotype with phenotype and build a model to predict the cell viability effects of kinase inhibitors. The first of these data sources is the large-scale PRISM cell viability screening effort. The PRISM data collection consists of a set of cell line viability measurements following exposure to a wide range of compounds(Yu et al., 2016) (Figure 1A). These compounds span multiple different target classes, but in this work we have focused on a specific subset of kinase inhibitors that have been independently assayed using the kinobead/MS-based method. This determines their precise kinase targets as well as the magnitude of inhibition of each kinase in response to

different concentrations of the inhibitors(Klaeger et al., 2017). Given that the compounds used in Klaeger et al. were all well known kinase inhibitors, most of the proteins that appear in the assay results are either known kinases or closely associated proteins. As such, we'll refer to the data originating from the Klaeger et al. result as "kinase inhibition states."

The primary challenge with combining these data sets is a lack of overlap between some of the concentrations used in the PRISM assay and those used by Klaeger et al. To overcome this problem, we used the viability curve fits provided by the PRISM database and imputed cell viability values for all of the concentrations used by Klaeger et al (Figure 1B). These cell viability results are represented as a value from 0-1, with 0 indicating complete cell death and 1 indicating no effect on cell viability. As expected, a majority of the treatments yielded little change in cell viability (Figure 1C). The distribution of cell viability values within each individual compound shows that while many of the compounds have minimal effects on cell viability, some compounds show a much wider range of cell viability effects (Figure 1D).

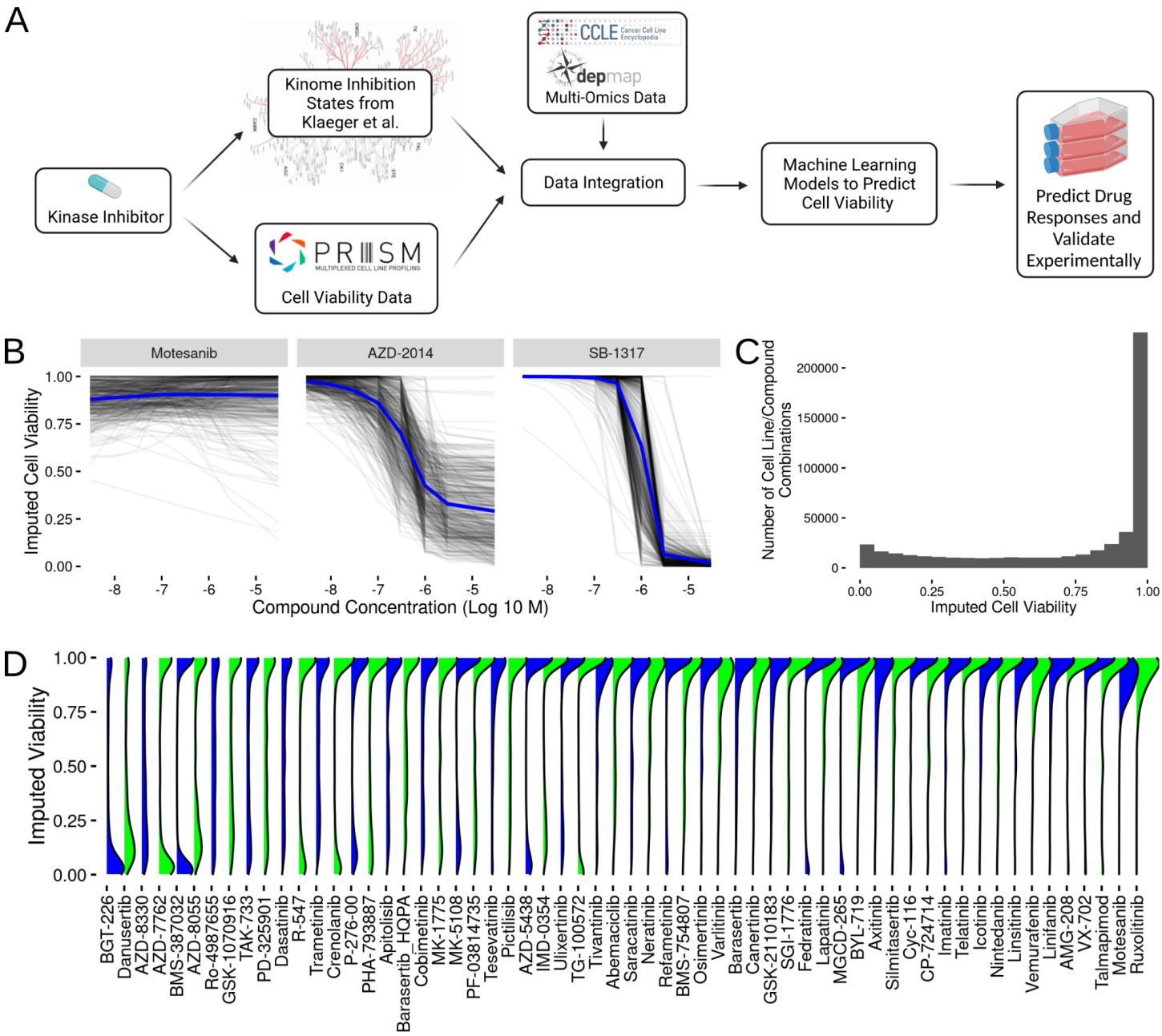

Figure 1: Study Design Overview and Imputation of Cell Viability from PRISM. (A) Flow chart showing data source collection, integration and modeling strategy. (B) Sample imputed cell viability curves for all assayed cell lines (gray underlying lines) and corresponding average imputed cell viability response (blue line) for three compounds showing low changes (Motesanib), medium level changes (AZD-2014) and high changes

(SB-1317) in cell viability. (C) Overall distribution of cell viability values imputed at Klaeger et al compound concentrations. (D) Distribution of imputed cell viability across all concentrations for a selection (60 out of 168) sampled evenly across the average imputed cell viability effect of the compounds present in both PRISM and the Klaeger et al set. The blue and green color scheme does not indicate anything about the underlying data and is meant to act as a visual aid for differentiating between adjacent curves.

After combining the PRISM and Klaeger et al. data sets, we have 168 compounds which have been assayed across 480 cell lines. We imputed the cell viabilities at each of the 8 concentrations used in the Klaeger et al. work, yielding about half a million treatment combinations across combinations of cell line, compound and concentration. With this data set, we also integrated the gene expression data available through the Cancer Cell Line Encyclopedia(Barretina et al., 2012). These gene expression values (log2 TPM values with a pseudocount of 1) were available in all but four of the 480 lines used in the PRISM compound screens. Following the integration of gene expression, we next examined how well single kinase inhibition and gene expression values were correlated with cell viability.

Cell Viability After Treatment with Kinase Inhibitors Shows Mild Correlation with Kinase inhibition state

Next, we investigated the relationship between kinase inhibition states (~520 proteins) and gene expression values with inhibitor-induced cell viability. To do this, we took each individual kinase inhibition state and gene expression value (~21,000 TPM values) and calculated the Pearson's correlation coefficient with the imputed cell viabilities (Figure 2A,B). These correlations were in general lower for the gene expression values, while the kinase inhibition state values showed both a higher average correlation and more variance (Figure 2C). This was not unexpected as the gene expression values are all characterized in unperturbed cell lines. Thus, as cell viability changes the gene expression values remain fixed, and any variation across gene expression must be correlated with broad changes in drug response between the cell lines. The examination of single correlation values gives a picture of how well related single expression or inhibition states are related to the cell viability phenotype.

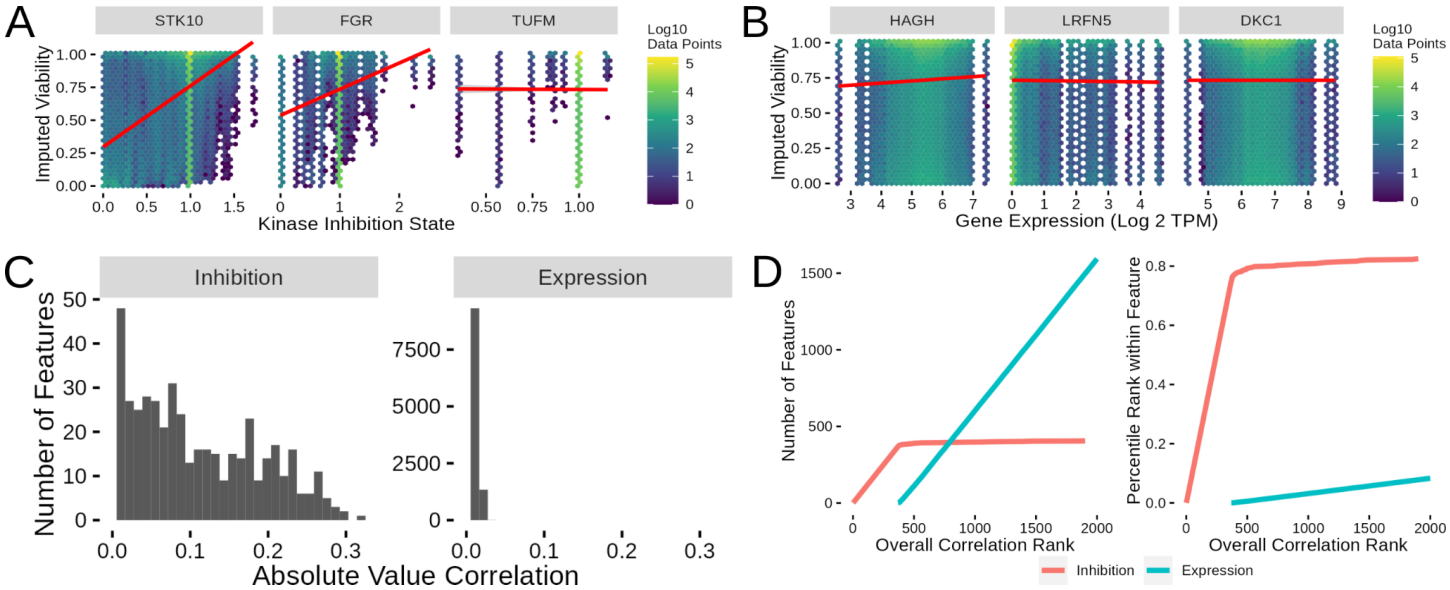

Figure 2: Single Feature Correlations Across Kinase inhibition and Gene Expression. (A) Sample kinase inhibition state versus imputed viability heatmap plots showing inhibition states with high (STK10), medium (FGR) and low (TUFM) correlation values. (B) Sample gene expression versus imputed viability heatmap plots showing genes with high (HAGH), medium (LRFN5) and low (DKC1) correlation values. (C) Overall distribution of correlations between kinase inhibition states and gene expression levels. (D) Plots showing what order classes of features are selected from the inhibition and expression correlations. The number of features from each class (left) selected at a given rank value and the percentage of the possible features (right) selected at a given feature selection rank cutoff.

While single features with correlation coefficient values in the ~0.3 range (the highest value observed in the kinase inhibition state data) will not produce sufficiently predictive models, the integration of multiple features may provide greater power. As such, we next sought to use the correlation values for feature selection. The most obvious way to use the correlation values is to put all the potential features (in this case, kinase inhibition state and gene expression) in correlation rank order and then select the top-X number of features for model inclusion. This produces differing sets of feature class counts and ratios depending on the number of features selected (Figure 2D right). Interestingly, the top ~350 features all come from the kinase inhibition states, with gene expression then starting to be included into the list above 350 features. As an alternative method to visualize the same selection process, we plotted what percent of a given feature class is included in the top list for the top 2000 features (Figure 2D left). This alternative view of the feature selection process shows that ~80% of the inhibition states are included in the model before gene expression starts to be included. This indicates that nearly all of the inhibition states are more highly correlated than the gene inhibition states and will thus be the sole factor considered for lower feature count models. Extending the feature list visualization to include lists greater than 2000 show that remaining inhibition states are slowly included as the top feature list expands (Figure S1A). This analysis of the structure of the single feature correlation results lays the groundwork for working with more sophisticated computational models to predict cell viability.

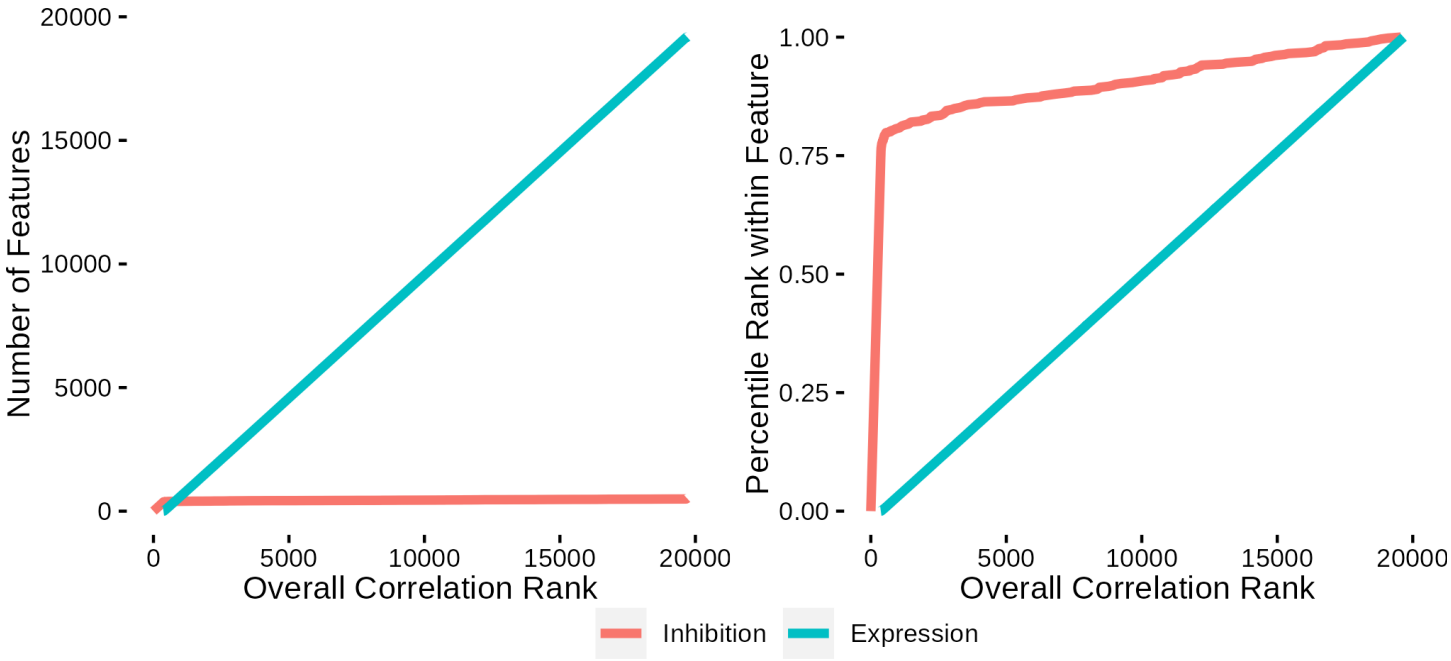

Supplemental Figure 1: Expanded Correlation Rankings (Associated with Figure 2). Extended version of Figure 2D covering all correlation ranks.

Computational Models Can Predict Cell Viability From a Combination of Kinase inhibition state and Gene Expression

With our initial analysis of the predictive power of single features from the Klaeger and gene expression data sets completed, we next moved to the development of models that integrated more than one feature with the end goal of predicting cell viability. To do this, we tested three types of models: linear regression, random forest and XGBoost. For our initial tests with these models, we used the default settings for all three model types and varied the number of features (either kinase inhibition states or gene expression values) provided to the model. Our cross validation strategy sought to balance our eventual goals of using the resulting models to make predictions about the cell viability effects in new cell lines and in untested compounds. As such, we choose a 10-fold cross validation strategy that randomized fold exclusion across the cell line-compound treatments (63767 total combinations) to improve the likelihood that our model testing results would be similar to downstream experiments. After producing the cross validation splits, we selected a specific number of features and built corresponding models (Figure 3A).

For benchmarking model performance, we built a naive model that simply guessed the average cell viability at each of the tested concentrations as a baseline for comparison (gray dotted lines in Figure 3A), and also compared results to previously run models on similar datasets(Corsello et al., 2020). Initially, we tested each model type with 100, 200, 300, 400, 500, 1000, 1500 and 2000 features. These preliminary tests showed that the random forest method performed the best at all of these feature counts and that performance (R^2 and RMSE) peaked at 500 features and out-performed our baseline dose-concentration-only model. To ensure that we had indeed found the peak in feature performance, we then tested 600, 700, 800 and 900 feature models and found that the 500 feature model was the peak (although all of these models performed very similarly). To better understand this model, we also looked more closely at the predicted versus actual imputed viability of the 500 feature random forest model (Figure 3B). This examination of the cross validation model results, showed that the average model performance was best at higher imputed viability values, while the predictions at lower imputed viabilities were not as accurate.

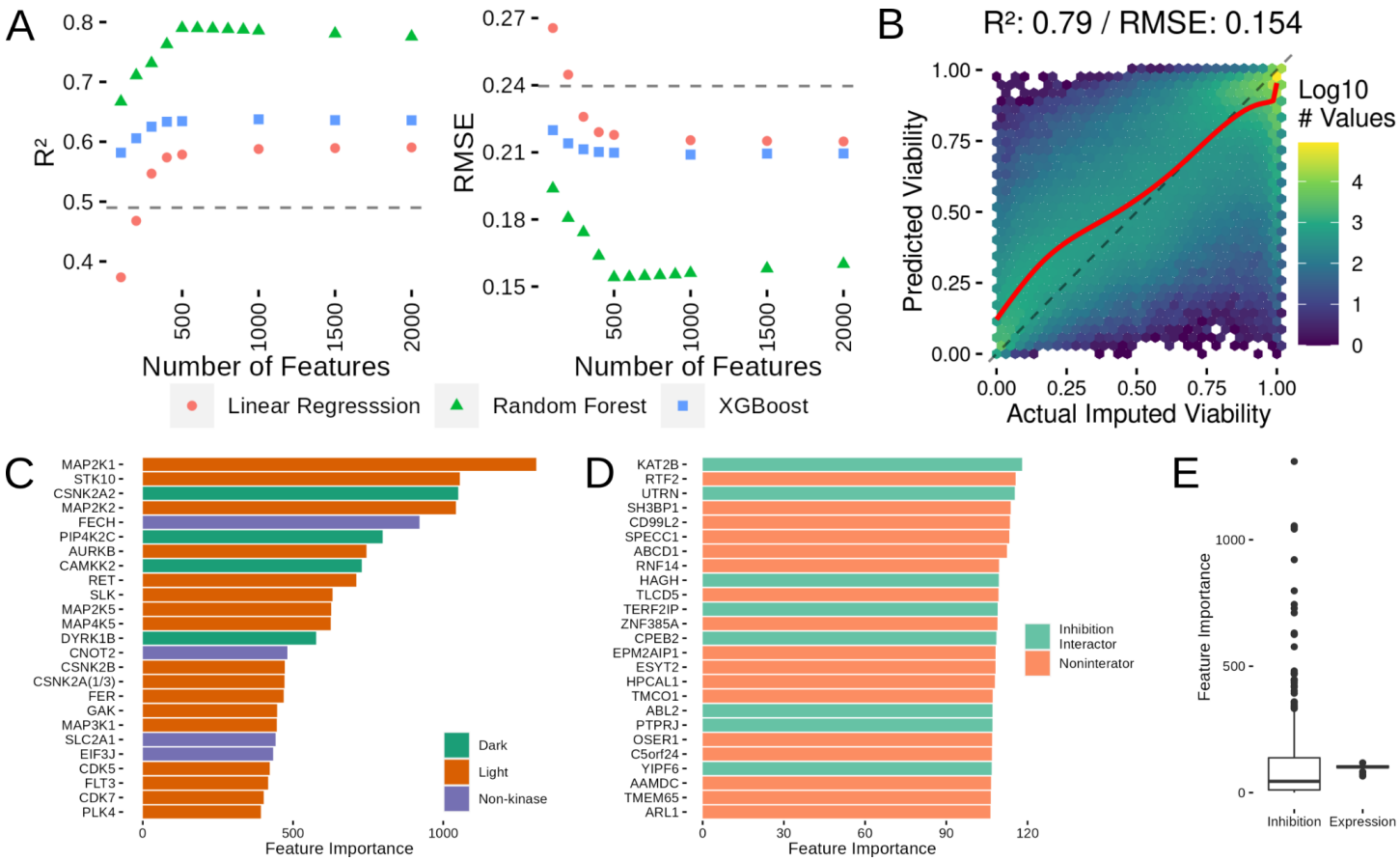

Figure 3: Development of a Regression Model to Predict Cell Viability and Assessment of Which Features Contribute to Model Predictions. (A) Comparison of R^2 and RMSE values from linear regression, random forest and XGBoost models. The gray dotted line shows the performance level of a dose-only model performance. (B) Actual imputed viability versus cross validated model predictions for the random forest model. The dashed line indicates where a perfect set of predictions would appear, while the red line shows a loess fit through the actual results. (C) Variable importance plot for the top 25 features in the final regression model. Each feature is prefixed with act or exp representing either kinase inhibition or gene expression respectively. (D) The top 25 most important expression features in the final model. (E) The overall distributions of feature importance values for the inhibition and expression features.

With random forest using 500 features selected as our best modeling strategy, we moved on to examining feature selection in the cross-validation models as well as parameter tuning. One concern with doing feature selection in each cross validation set was that there would be a large amount of volatility in feature selection between each cross validation model run. We found that in each of the cross validation runs, at least 75% of the features are included in all of the feature selection sets (Figure S2A). To ensure that the default random forest parameter models were near the optimal tuning, we also tested cross-validated models with 1000, 1500

and 2000 trees (500 trees is the default value). Increasing the tree count had little effect on model quality (Figure S2B), so we opted to use the default value of 500 trees.

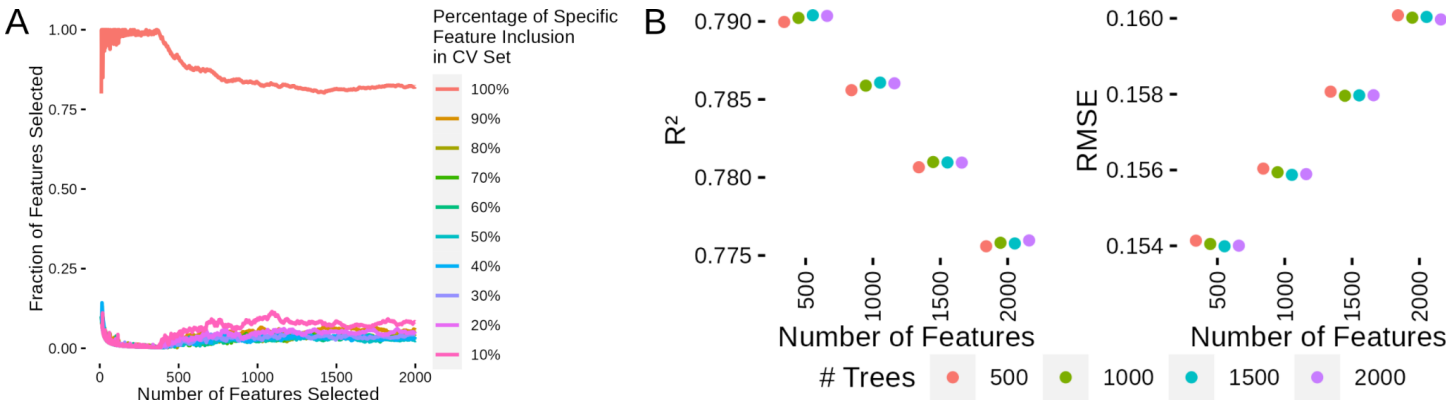

Supplemental Figure 2: Feature Selection with Cross Validation and Assessment of Increasing Random Forest Trees (Associated with Figure 3). (A) The effect of cross validation data division on which features are selected for model inclusion. (B) The effect on R^2 and RMSE of increasing the number of trees used in the random forest algorithm.

Our first step in building the final kinase inhibition and gene expression model, was to first select the 500 features that would be included in the model. Using the same correlation ranking scheme used in our cross validated models, 390 out of 520 kinase inhibition states and 110 out 19177 gene expression features were selected for model inclusion. We next built the final random forest model with the full data set and collected variable importance metrics for each of the included features. In order to understand the kinase and non-kinases included in the selected inhibition states, we classified each protein as either a non-kinase or as a well-studied (Light) or understudied (Dark) kinase (Figure 3C)(Berginski et al., 2020). Several of these genes have well-known roles in cell viability and cancer, including MAP2K1 (MEK1), AURKB and CDK7. Interestingly, the model also identifies several understudied kinases, CSNK2A2, PIP4K2C, CAMKK2 and DYRK1B, as being influential in the model's cell viability predictions. To better contextualize the expression values included in the model, we used the STRING database to see how many of the selected genes interacted with the proteins included in the inhibition features (Figure 4D). Of the 110 genes included in the expression values, 40 interact with at least one protein in the inhibition set and the average expression gene interacts with 1.7 inhibition state genes. In comparison to 10,000 randomly drawn expression gene sets of size 110, 84% interact with fewer than 40 inhibition states and 80% have a lower average inhibition gene interactor count below 1.7. The global view of the variable importance metrics also shows that nearly all of the expression features have similar importance values in the final random forest model (Figure 3E). We next attempted to better understand how the interaction between inhibition states and gene expression levels affected model performance.

The Combination of Kinase Inhibition States and Baseline Gene Expression Produces the Best Results

After thoroughly examining the results of the inhibition state and gene expression combined model, we next wanted to investigate how the model would perform when we excluded certain parts of the full data set. Using the same 10-fold feature selection cross validation strategy and the same cross validation fold splits described above, we rebuilt the model using only inhibition state or only gene expression (Figure 4A). The gene-expression-only models performed very poorly (R^2 of ~0.01 and RMSE of 0.33), which was expected due to the fact that the gene expression values are fixed and do not vary with the compound concentrations. When we built models using the inhibition states alone, we observed identical performance for feature counts 300 and below. This was also expected as the correlational feature selection methods always select inhibition features for the first ~350 features. With feature counts of 400 and 500, we observed that the additional information provided by the gene expression features began to improve the model (0.05 improvement in R^2 and a 0.02 decrease in RMSE). Thus, while the expression features alone are not sufficient to predict cell viability, they do provide an appreciable improvement in the model performance in combination with inhibition features.

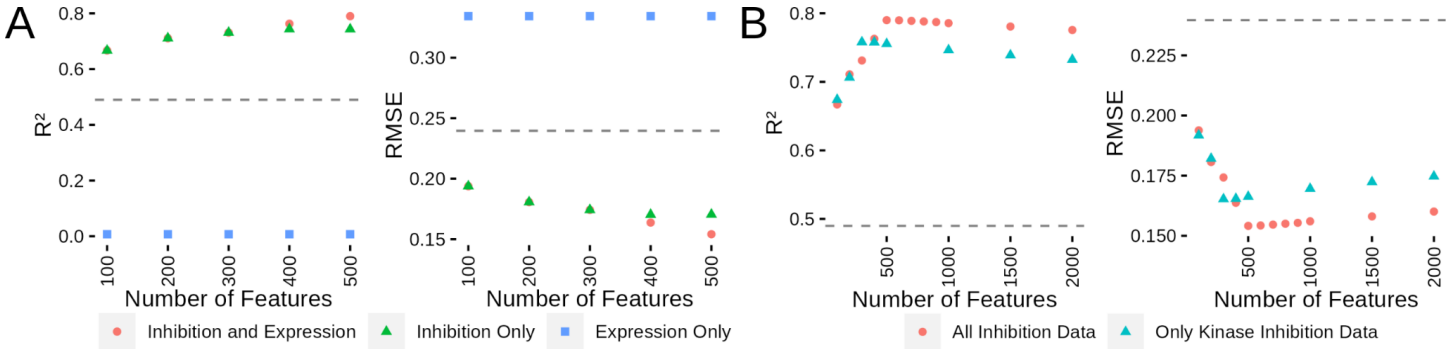

Figure 4: Model Performance is Best with Access to All Inhibition States and Gene Expression Values. (A) Comparison of R^2 and RMSE performance for models using only expression, only inhibition or inhibition and expression features. (B) Comparison of R^2 and RMSE performance for models using gene expression and all inhibition data or only the kinase subset.

Having established that both inhibition and expression data are needed for the best model performance, we next investigated how the non-kinases in the inhibition data set affected model performance. This question is an interesting avenue to explore as, while the Klaeger et al. study was confined to kinase inhibitors, the presence of ~50% non-kinase proteins inspired us to assess how the model would perform without the non-kinases. We rebuilt the inhibition data set and ran the same modeling methodology including the gene expression values to allow us to compare to our previous models (Figure 4B). The optimum kinase-only inhibition data model had a maximum R^2 of 0.76 and a RMSE of 0.17 (compared to R^2 of 0.79 and RMSE of 0.15 for the full set). These results indicate that the non-kinases are providing some additional information that the model is able to use, which is in agreement with the presence of non-kinases in the top 25 of the variable importance metrics (Figure 3C). Having fully examined the kinase inhibition state and expression model, we next investigated if any of the other multiomics data sets available could improve upon these models.

Models Only Show Mild Improvement from Inclusion of a Broad Spectrum of Omics Data

Gene expression is only one of several different types of comprehensive data that has been collected for many of the cell lines used in the PRISM assay. These additional data sets include:

- DepMap CRISPR-KO screening: genome-wide gene knockout viability measurements (DepMap Score)
- Copy-number-variation: gene level copy number variation (CNV)
- Whole Genome Proteomics: mass spectroscopy-based measurement of relative protein abundance (proteomics)

Given the broad and complementary nature of these data sets, we investigated whether we could integrate these data sets to improve upon the kinase inhibition and gene expression models we described above. The Depmap, CNV and proteomics data sets all overlap with a different number of cell lines present in the PRISM data set (Figure S3A). All of the data sets are available for 212 cell lines (gene expression is available for 476 cell lines represented in PRISM). We focused our modeling efforts on these 212 cell lines to ensure that a complete collection of data was available. We followed the same strategy as in the above modeling effort where we first investigated the correlation between single features and cell viability. The 212 cell line subset showed very similar correlation distributions between kinase inhibition and gene expression (Figure S3B). The newly added feature (CNV, DepMap scores and proteomics) correlations, had correlation distributions very similar to gene expression (Figure S3B). Using the correlation feature ranking, we also determined which features would be included in models of various sizes (Figure 5A and Figure S3C). With these data sets organized and our feature selection techniques specified, we tested how inclusion of these data sets affected model quality.

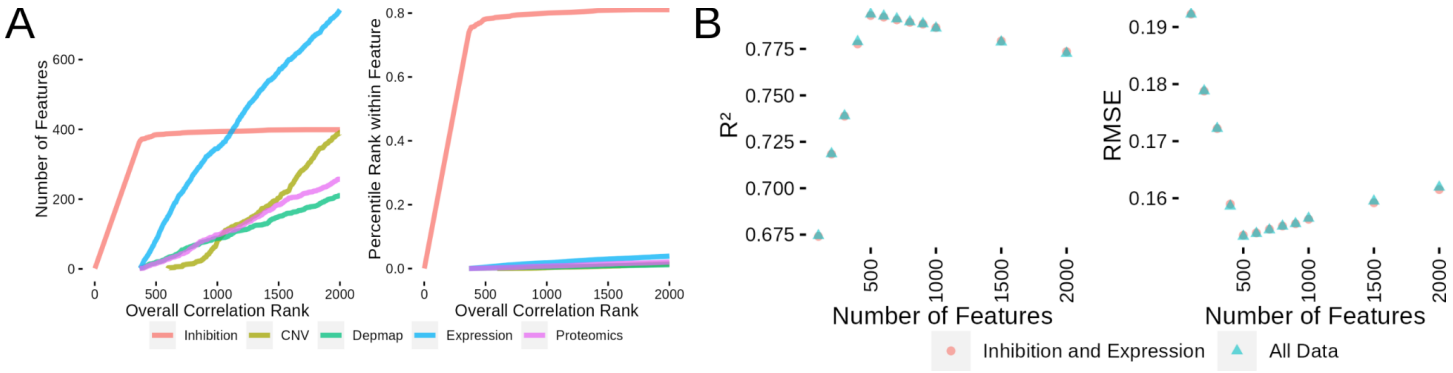

Figure 5: Regression Models using Additional Data Sets Don't Dramatically Outperform inhibition and Expression Models. (A) Plot showing the order features are selected for model inclusion (left) and the percentile rank within each feature class as features are selected for inclusion in the model (right). (B) Comparison between models built with inhibition data and expression or all available data sets by R^2 (left) and by RMSE (right).

Based on our previous experience with building the kinase inhibition and expression models, we decided to only test the best-performing random forest method. We also used the same 10-fold cross validation across the cell line/compound combinations. This resulted in higher instability in feature inclusion across the cross validation folds (Figure S3D). As shown in Figure 5B, integration of these other data sets led to performance that was nearly identical to the model with only kinase inhibition and gene expression. The peak performance was achieved at 500 features in both model variants with R^2 values of 0.794 (0.153 RMSE) and 0.793 (0.154 RMSE) for the all data and inhibition/expression models respectively. This indicates that gene expression values alone contain substantially similar information as the remaining set of multiomics data. Given our desire to build a model which uses the most easily reproducible data sets and only minor improvements were observed with the full data collection, we decided to move forward with the integrated model combining kinase inhibition states and gene expression values.

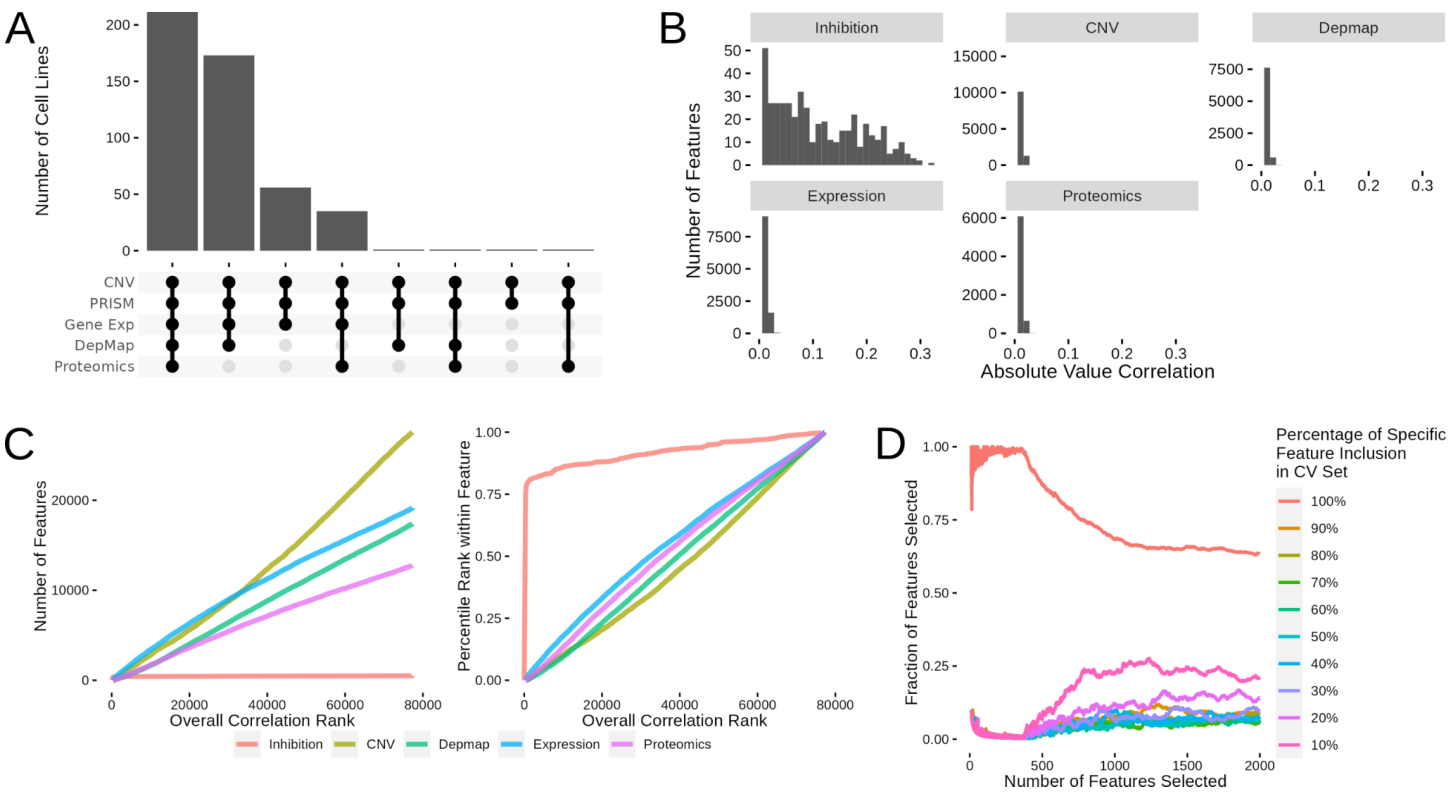

Supplemental Figure 3: Expanded Correlation Rankings and Effect of Cross Validation Subsetting on Feature Selection (Associated with Figure 5) (A) Upset plot showing the overlap between data sets across cell lines in the PRISM assay. (B) Small multiples plot showing the correlation of individual features to imputed

cell viability for each of the feature types considered in this model. (C) Full feature correlation rankings for all data set types considered for Figure 5. (D) Effect of random 10-fold cross validation subsetting on which features are included in what percentage of the cross validation data sets.

Validating the Models was Successful within the Our Ability to Replicate Previous PRISM Results

With the model production decisions finalized, we then applied this model to the untested cell line and compound combinations. The final model was produced using the 63189 cell line and compound combinations with interpolated viability values (Figure 6A). Of the data that went into model production, 476 cell lines and 168 compounds were represented. This left 903 cell lines in the CCLE gene expression data set and 61 Kleager kinase inhibitors that have not been tested in the PRISM viability assays (in addition to a few other untested combinations) where we were able to apply our model to predict cell viability at each of the compound concentrations used in the Klaeger assay. Ultimately, this resulted in us producing predictions for about 250,000 cell line and compound combinations (Sup Data 1). We hope that providing these prediction results will enable other researchers to find interesting or unexpected compounds that target specific cancer types. For the work presented here, we focused our validation efforts on a subset of breast cancer cell lines.

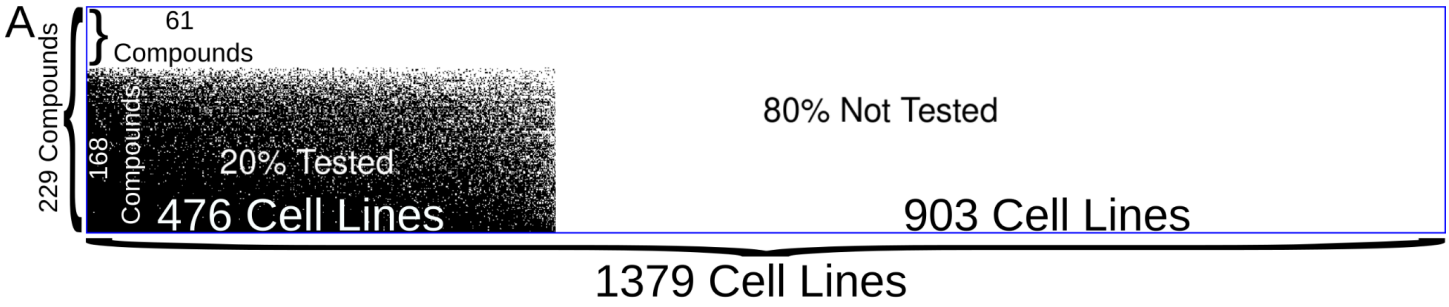

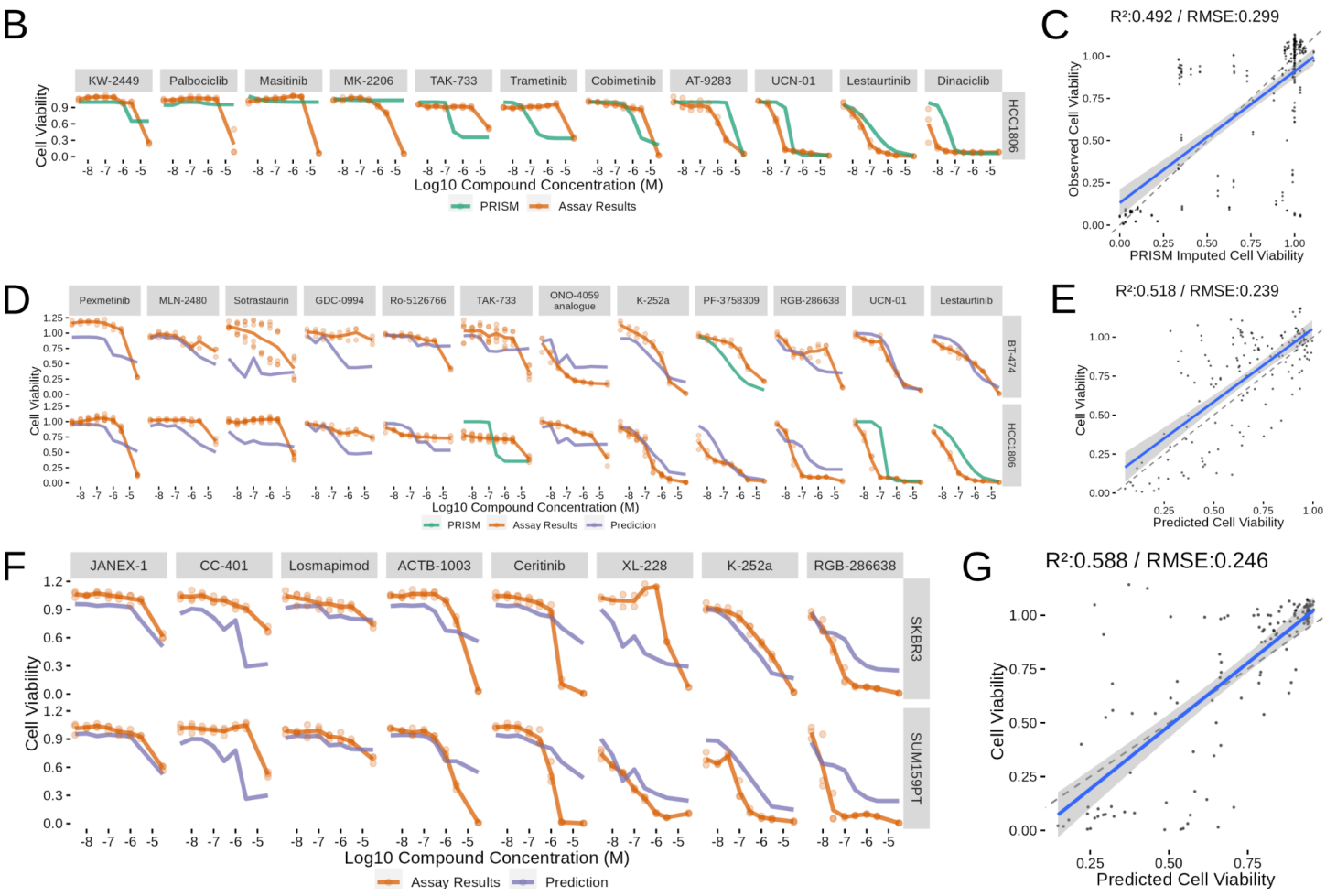

Figure 6: Validating a Subset of Compound Predictions in Breast Cancer Cell Lines. (A) Visualization of the space of compound (Y-axis) and cell line (X-axis) combinations that have been tested (white) and non tested (black) with a blue box surrounding the entire visualization. (B) Cell viability results from testing a set of compounds (labeled above each curve) and a cell line (HCC1806) already tested in the PRISM collection. (C) Scatterplot summarizing all the results from part B into a single plot with a linear best fit line showing in blue. (D) Cell viability results and corresponding predictions or PRISM results from a set of cell lines included in PRISM (BT-474 and HCC1806) and a selection of compounds which were mostly not included in PRISM. (E) Scatterplot summarizing all the prediction results from part D into a single plot. (F) Cell viability results and corresponding predictions for a set of cell lines and compounds not included in PRISM. (G) Scatterplot summarizing all the results from part F into a single plot.

Our first goal when beginning to validate a subset of model predictions was to see how well we could replicate the results from the PRISM assay. We selected the well characterized triple negative breast cancer (TNBC) cell line HCC1806 and a set of compounds that displayed a range of viability effects from the 134 Kleager kinase inhibitors that had been used in the PRISM assay with the HCC1806 cell line (Figure 6B). Several of these compounds performed very similarly in our assay as compared with the imputed viability PRISM values, notably Cobimetinib, UCN-01, AT-9283, Lestauritinib and Dinaciclib. However, several of the compounds that showed high viability effects at high concentrations were not reflected in the imputed viability results, which lowered the replication R^2 to 0.492 and the RMSE to 0.299 (Figure 6C). With the limitations identified by the replication effort acknowledged, we next moved into testing new cell line and compound combinations.

We started testing new cell line and compound combinations by continuing with the HCC1806 line and adding in the HER2 positive breast cancer cell line BT-474. We selected a set of compounds predicted to have a range of effects on the two cell lines and then conducted a viability screen with each of these compounds (Figure 6D). Much like the replication attempt, we observed several compounds where the predicted viabilities were close to the measured viability (K-252a, UCN-01, PF-3758309 and Lesauritinib). Overall, the R^2 (0.518) and RMSE (0.239) values were comparable with replication effort, indicating that the model was performing well on new compounds (Figure 6E). As our most challenging final test, we decided to test two cell lines that are not present in the PRISM data set (HER2+ line SKBR3 and TNBC line SUM159PT) against a set of compounds that weren't included in the PRISM compound set. Once again, with this "double-untested" experiment, we selected a set of compounds predicted to have varying effects across concentrations and observed a combination of compounds with strong and weak correlation between predictions and results (Figure 6F). Notable among the better results were JANEX-1, Losmapimod and K-252a, while the model struggled with CC-401 and parts of the RGB-286638, ACTB-1003 and Ceritinib curves. The overall performance of the model (R^2 of 0.588 and RMSE of 0.246) were comparable to the other model validation results (Figure 6G). These independent validation efforts demonstrate that the model predictions are able to generalize into previously untested cell lines and compounds.

Discussion

Given the potential of targeted kinase inhibitor therapies, the ability to predict how a given treatment may alter kinome state and lead to a given phenotype is fundamentally enabling. In this work, we developed a set of computational models that predict cell viability after treatment with a set of small molecule kinase inhibitors. To accomplish this, we used several publicly available data sets that provided information concerning the untreated gene expression of the cell lines used in the viability screen and another that gave detailed information about the proteins targeted by small molecule kinase inhibitors. We examined how single gene expression and kinome state values were related to cell viability and how models with various numbers of gene expression and kinome state values varied in quality. In addition to gene expression, we also tested a set of models which included a broader range of baseline measurements (CNV, proteomics and gene essentiality) and concluded that these additional data sets were not able to significantly improve model performance. Finally, we tested some of the model predictions in several triple negative and HER2 positive breast cancer lines and found acceptable agreement between the model predictions and these results.

This work demonstrates how generic knowledge of the kinome can predict a cellular process as fundamental as viability. Importantly, the models achieved these surprising results by using a "generic" or "general" kinase

inhibition profile measured with proteomic kinobead profiling of a four cell line lysate exposed to an extensive library of kinase inhibitors at multiple doses(Klaeger et al., 2017). Thus, the models learned by linking non-cell line specific kinome inhibition state information with that of specific drug-cell line relationships.

We also hope that by providing a full set of viability predictions for the broad range of cancer cell lines covered by the CCLE that this work can act as a resource for other researchers to find unexpected or interesting kinase inhibitors that affect their most used cell line model systems. We would also like to acknowledge several limitations of this work. All of the results in this paper rest on the availability of kinome profiling data specific to a given kinase inhibitor, so the methods here are not applicable to prediction of cell viability effects in any other class of compound. We believe that a similar strategy could be used to build models in compound classes where the spectrum of targets were as comprehensively identified. The universe of small molecule kinase inhibitors is substantially larger than those that were surveyed by Klaeger et al., but since our modeling methodology depends on the comprehensive nature of their work, we're limited in the number of compounds where we can make predictions. One of our next goals is to attempt to broaden the scope of compounds through integration of other high-content kinome profiling techniques such as KinomeScan and Nano-BRET. In addition, while the models described in this paper do make somewhat accurate predictions, these results point to a degree of missing predictability in cell viability for which new methods and data will need to be developed and collected.

This work also suggests several extensions that would broaden or improve the model. Given recent interest in finding new compound combinations computationally, we are beginning to examine how best to combine the information from multiple compound kinome inhibition states to predict the resulting cell viability effects. This would allow us to run computational drug combination screens. In addition, the methods outlined here will also likely work for any phenotype that can be measured after treatment with small molecule inhibitors and with sufficient throughput to gather a large enough data set. Finally, while we have made all of the code and data necessary to reuse our models available to the public on github, we also acknowledge that this is not the most user-friendly method for allowing non-computationally minded users to access the model. Thus, we also plan on developing a web-based system for allowing non-computationally minded users to submit a gene expression profile and receive a set of predictions concerning how their cellular system is expected to respond to the Klaeger set of kinase inhibitors.

Overall, we hope that this paper makes a contribution to our understanding of how the overall state of kinome in response to small molecule inhibitors contributes to cell viability phenotypes. Our findings demonstrate that while individual kinase inhibition states and other single gene or protein readings are not very predictive of cell viability, machine learning approaches are able to combine sets of measurements related to the small molecule kinase inhibitors and gene expression data to make cell viability predictions. The results presented here show how a thorough understanding of kinase activity levels in conjunction with baseline omics data can be used to gain a better understanding of cell viability.

Methods

Our methods can be divided into two parts describing the computational aspects of this work and the experimental methods used to test the output of the computational components.

Data Sources

We used two primary data sources for this paper: the supplemental data section from Klaeger et al.(Klaeger et al., 2017) and the cell viability screening results from the PRISM lab. Specifically, we collected and organized the kinase inhibition states from supplemental table 2 of Klaeger et al, focusing on the Kinobeads subsheet. As for the PRISM data, we used the data from 2019 Q4 (labeled 19Q4 in the depmap portal), specifically the secondary screening data. In addition to these two data sets, we used supplemental data sets from the CCLE(Barretina et al., 2012) and DepMap(Tsherniak et al., 2017). These data included results from baseline RNAseq (CCLE_expression.csv), copy number variation (CNV, CCLE_gene_cn.csv) and CRISPR-KO viability screening (CRISPR_gene_effect.csv). The 2021Q3 versions of these files were used. The proteomics data was downloaded from the Gygi lab website (https://gygi.hms.harvard.edu/publications/ccle.html), specifically

Table S2 (Nusinow et al., 2020). We also used version 11.5 of the STRING (Szklarczyk et al., 2021) protein network database (9606.protein.links.v11.5.txt.gz).

Data Preprocessing

The scripts implementing these descriptions are all available through github.

Klaeger et al. Kinase Inhibition Profiles: We read the values from the supplemental data table into R and produced a list of all proteins observed in any of the kinase inhibitor treatments. Since this table only contains the proteins affected by each compound, we filled in the relative intensity values for genes not associated with a given inhibitor with the default value of 1. There was a small (1.8%) number of single concentration values missing from the listed affected proteins, so we filled these values as the average of two nearest concentrations. Finally, a smaller set (0.01%) of likely outlier relative intensity readings were truncated to the 99.99 percentile (3.43).

PRISM Cell Viability: Since relatively few of the concentrations used in the PRISM assay match those used by Klaeger et al., we opted to use the response curve parameters provided through the depmap portal to interpolate the cell viability values. We interpolated these values at 30 μM, 3 μM, 1 μM, 300 nM, 100 nM, 30 nM, 10 nM and 3 nM to match those used by Klaeger et al. We applied a filter to remove any response curve parameter set that indicated that a given cell line and compound combination produced enhanced cell growth with increasing compound concentration. To perform the viability extrapolation, we used the four-parameter log-logistic formula described in the drc R package(Ritz et al., 2015).

Gene Expression, CNV, CRISPR-KO and Proteomics: The files provided by the depmap portal for gene expression, CNV and CRISPR-KO values required very little modification to work in our machine learning pipelines. The primary modification was to add identifiers to each gene label, to ensure that omics data related to the same gene weren't accidentally combined. The CRISPR-KO data also required an additional filter to remove 10 cell lines with missing data. The proteomics data processing was slightly more complicated, as there were substantially more protein readings missing from many more lines. In the cases of missing protein readings, we imputed these values to the minimum value for the overall distribution of that protein minus one standard deviation.

String: The STRING database(Szklarczyk et al., 2021) also required only mild preprocessing to extract the proteins that interacted with the components of our models. We filtered the interaction list to the high confidence (above 0.7) set and used bioMart(Durinck et al., 2009) to convert the Ensemble protein identifiers to HGNC identifiers for matching with the other data sets.

Modeling Techniques and Types

To assess our models we used a 10-fold cross validation strategy which randomized training and test set inclusion across the cell line and compound combinations. Thus, for any given viability curve resulting from treatment of a cell line with a compound, all of the results from the assay were considered as one unit for cross validation purposes. All steps of feature selection were also conducted under this cross validation framework as well. For every fold of our data, we recalculated the correlation coefficient between cell viability and the features available to the model (kinase inhibition state, gene expression, etc) using only the data in the training set. The number of features was varied as specified in the results section. We used the entire data set to build the final model used to make the predictions in Supplemental Data File 1 and the results displayed in Figure 6.

We used random forest, XGBoost and linear regression for all of our modeling efforts. All of our models are implemented using the tidymodels framework in R. We used the ranger random forest engine(Wright and Ziegler, 2017), the default XGBoost engine(Chen and Guestrin, 2016) and the default linear regression engine. After selecting random forest as our primary modeling method, we also tuned the number of trees.

Compound Testing

BT-474, HCC1806, SUM-159 and SKBR-3 cells were grown in ATCC recommended media and seeded at 4000, 2000, 4000 and 500 cells per well respectively, in white flat-bottom 96-well plates (Corning). 24 hours after seeding, cells were treated with the respective drugs prepared in DMSO. All drugs were dosed at the same eight concentrations used in the Klaeger study: 30 μM, 3 μM, 1 μM, 300 nM, 100 nM, 30 nM, 10 nM and 3 nM. Seventy-two hours post-treatment, cells were lysed with CellTiter-Glo (Promega) per the manufacturer's protocol. Luminescence was read using the PHERAstar FS microplate reader (BMG Labtech) and gain adjustments were conducted for each cell line. Data were normalized row-wise to the DMSO-only (0.5% on cells) control samples on each plate to calculate relative viability. Quality checks were performed to look at the data distribution and the presence of spatial bias on a plate. A quality control metric of <120% of DMSO was applied to all rows analyzed. Across all >150 rows analyzed, only one row of XL-228 treated SKBR-3 cells failed to meet this criteria and was removed from analysis.

Software and Data Availability

All of the code written to support this paper is available through github (https://github.com/gomezlab/kinotype_viability) along with a walkthrough explaining where to find the code relevant to each part of the paper. We have also made all of the model validation results available through zenodo (https://doi.org/10.5281/zenodo.6323686).

Acknowledgements

We would like to thank Donglin Zeng for helpful discussions concerning feature selection techniques, UNC Research Computing for access to the computational resources necessary for this work. We would also like to thank Madison Jenner and Jen Jen Yeh for providing a sample of JANEX-1.

Funding

National Institutes of Health (5U24DK116204)
- Matthew Berginski
- Chinmaya Joisa
- Shawn Gomez

Attwood MM, Fabbro D, Sokolov AV, Knapp S, Schiöth HB. 2021. Trends in kinase drug discovery: targets, indications and inhibitor design. *Nat Rev Drug Discov* **20**:839–861.

Bantscheff M, Eberhard D, Abraham Y, Bastuck S, Boesche M, Hobson S, Mathieson T, Perrin J, Raida M, Rau C, Reader V, Sweetman G, Bauer A, Bouwmeester T, Hopf C, Kruse U, Neubauer G, Ramsden N, Rick J, Kuster B, Drewes G. 2007. Quantitative chemical proteomics reveals mechanisms of action of clinical ABL kinase inhibitors. *Nat Biotechnol* **25**:1035–1044.

Barretina J, Caponigro G, Stransky N, Venkatesan K, Margolin AA, Kim S, Wilson CJ, Lehár J, Kryukov GV, Sonkin D, Reddy A, Liu M, Murray L, Berger MF, Monahan JE, Morais P, Meltzer J, Korejwa A, Jané-Valbuena J, Mapa FA, Thibault J, Bric-Furlong E, Raman P, Shipway A, Engels IH, Cheng J, Yu GK, Yu J, Aspesi P Jr, de Silva M, Jagtap K, Jones MD, Wang L, Hatton C, Palescandolo E, Gupta S, Mahan S, Sougnez C, Onofrio RC, Liefeld T, MacConaill L, Winckler W, Reich M, Li N, Mesirov JP, Gabriel SB, Getz G, Ardlie K, Chan V, Myer VE, Weber BL, Porter J, Warmuth M, Finan P, Harris JL, Meyerson M, Golub TR, Morrissey MP, Sellers WR, Schlegel R, Garraway LA. 2012. The Cancer Cell Line Encyclopedia enables predictive modelling of anticancer drug sensitivity. *Nature* **483**:603–607.

Berginski ME, Moret N, Liu C, Goldfarb D, Sorger PK, Gomez SM. 2020. The Dark Kinase Knowledgebase: an online compendium of knowledge and experimental results of understudied kinases. *Nucleic Acids Res*. doi:10.1093/nar/gkaa853

Bhullar KS, Lagarón NO, McGowan EM, Parmar I, Jha A, Hubbard BP, Rupasinghe HPV. 2018. Kinase-targeted cancer therapies: progress, challenges and future directions. *Mol Cancer* **17**:48.

Chen T, Guestrin C. 2016. XGBoost: A Scalable Tree Boosting SystemProceedings of the 22nd ACM SIGKDD International Conference on Knowledge Discovery and Data Mining, KDD '16. New York, NY, USA: Association for Computing Machinery. pp. 785–794.

Cohen P, Cross D, Jänne PA. 2021. Kinase drug discovery 20 years after imatinib: progress and future directions. *Nat Rev Drug Discov* **20**:551–569.

Collins KAL, Stuhlmiller TJ, Zawistowski JS, East MP, Pham TT, Hall CR, Goulet DR, Bevill SM, Angus SP, Velarde SH, Sciaky N, Oprea TI, Graves LM, Johnson GL, Gomez SM. 2018. Proteomic analysis defines kinase taxonomies specific for subtypes of breast cancer. *Oncotarget* **9**:15480–15497.

Corsello SM, Nagari RT, Spangler RD, Rossen J, Kocak M, Bryan JG, Humeidi R, Peck D, Wu X, Tang AA, Wang VM, Bender SA, Lemire E, Narayan R, Montgomery P, Ben-David U, Garvie CW, Chen Y, Rees MG, Lyons NJ, McFarland JM, Wong BT, Wang L, Dumont N, O'Hearn PJ, Stefan E, Doench JG, Harrington CN, Greulich H, Meyerson M, Vazquez F, Subramanian A, Roth JA, Bittker JA, Boehm JS, Mader CC, Tsherniak A, Golub TR. 2020. Discovering the anti-cancer potential of non-oncology drugs by systematic viability profiling. *Nat Cancer* **1**:235–248.

Daemen A, Griffith OL, Heiser LM, Wang NJ. 2013. Modeling precision treatment of breast cancer. *Genome Biol*.

Deininger M, O'Brien SG, Guilhot F, Goldman JM, Hochhaus A, Hughes TP, Radich JP, Hatfield AK, Mone M, Filian J, Reynolds J, Gathmann I, Larson RA, Druker BJ. 2009. International Randomized Study of Interferon Vs STI571 (IRIS) 8-Year Follow up: Sustained Survival and Low Risk for Progression or Events in Patients with Newly Diagnosed Chronic Myeloid Leukemia in Chronic Phase (CML-CP) Treated with Imatinib. *Blood* **114**:1126.

Duncan JS, Whittle MC, Nakamura K, Abell AN, Midland AA, Zawistowski JS, Johnson NL, Granger DA, Jordan NV, Darr DB, Usary J, Kuan P-F, Smalley DM, Major B, He X, Hoadley KA, Zhou B, Sharpless NE, Perou CM, Kim WY, Gomez SM, Chen X, Jin J, Frye S V, Earp HS, Graves LM, Johnson GL. 2012. Dynamic reprogramming of the kinome in response to targeted MEK inhibition in triple-negative breast cancer. *Cell* **149**:307–321.

Durinck S, Spellman PT, Birney E, Huber W. 2009. Mapping identifiers for the integration of genomic datasets with the R/Bioconductor package biomaRt. *Nat Protoc* **4**:1184–1191.

Falzone L, Salomone S, Libra M. 2018. Evolution of Cancer Pharmacological Treatments at the Turn of the Third Millennium. *Front Pharmacol* **9**:1300.

Frejno M, Zenezini Chiozzi R, Wilhelm M, Koch H, Zheng R, Klaeger S, Ruprecht B, Meng C, Kramer K, Jarzab A, Heinzlmeir S, Johnstone E, Domingo E, Kerr D, Jesinghaus M, Slotta-Huspenina J, Weichert W, Knapp S, Feller SM, Kuster B. 2017. Pharmacoproteomic characterisation of human colon and rectal cancer. *Mol Syst Biol* **13**:951.

Geyer CE, Forster J, Lindquist D, Chan S, Romieu CG, Pienkowski T, Jagiello-Gruszfeld A, Crown J, Chan A, Kaufman B, Skarlos D, Campone M, Davidson N, Berger M, Oliva C, Rubin SD, Stein S, Cameron D. 2006. Lapatinib plus capecitabine for HER2-positive advanced breast cancer. *N Engl J Med* **355**:2733–2743.

Ghandi M, Huang FW, Jané-Valbuena J, Kryukov GV, Lo CC, McDonald ER 3rd, Barretina J, Gelfand ET, Bielski CM, Li H, Hu K, Andreev-Drakhlin AY, Kim J, Hess JM, Haas BJ, Aguet F, Weir BA, Rothberg MV, Paolella BR, Lawrence MS, Akbani R, Lu Y, Tiv HL, Gokhale PC, de Weck A, Mansour AA, Oh C, Shih J, Hadi K, Rosen Y, Bistline J, Venkatesan K, Reddy A, Sonkin D, Liu M, Lehar J, Korn JM, Porter DA, Jones MD, Golji J, Caponigro G, Taylor JE, Dunning CM, Creech AL, Warren AC, McFarland JM, Zamanighomi M, Kauffmann A, Stransky N, Imielinski M, Maruvka YE, Cherniack AD, Tsherniak A, Vazquez F, Jaffe JD, Lane AA, Weinstock DM, Johannessen CM, Morrissey MP, Stegmeier F, Schlegel R, Hahn WC, Getz G, Mills GB, Boehm JS, Golub TR, Garraway LA, Sellers WR. 2019. Next-generation characterization of the Cancer Cell Line Encyclopedia. *Nature* **569**:503–508.

Golkowski M, Lau H-T, Chan M, Kenerson H, Vidadala VN, Shoemaker A, Maly DJ, Yeung RS, Gujral TS, Ong S-E. 2020. Pharmacoproteomics Identifies Kinase Pathways that Drive the Epithelial-Mesenchymal Transition and Drug Resistance in Hepatocellular Carcinoma. *Cell Syst*. doi:10.1016/j.cels.2020.07.006

Keefe DMK, Bateman EH. 2019. Potential Successes and Challenges of Targeted Cancer Therapies. *J Natl Cancer Inst Monogr* **2019**. doi:10.1093/jncimonographs/lgz008

Klaeger S, Heinzlmeir S, Wilhelm M, Polzer H, Vick B, Koenig P-A, Reinecke M, Ruprecht B, Petzoldt S, Meng C, Zecha J, Reiter K, Qiao H, Helm D, Koch H, Schoof M, Canevari G, Casale E, Depaolini SR, Feuchtinger A, Wu Z, Schmidt T, Rueckert L, Becker W, Huenges J, Garz A-K, Gohlke B-O, Zolg DP, Kayser G, Vooder T, Preissner R, Hahne H, Tõnisson N, Kramer K, Götze K, Bassermann F, Schlegl J, Ehrlich H-C, Aiche S, Walch A, Greif PA, Schneider S, Felder ER, Ruland J, Médard G, Jeremias I, Spiekermann K, Kuster B. 2017. The target landscape of clinical kinase drugs. *Science* **358**. doi:10.1126/science.aan4368

Lahiry P, Torkamani A, Schork NJ, Hegele RA. 2010. Kinase mutations in human disease: interpreting genotype–phenotype relationships. *Nat Rev Genet* **11**:60–74.

Laufer S, Bajorath J. 2022. New Horizons in Drug Discovery - Understanding and Advancing Different Types of Kinase Inhibitors: Seven Years in Kinase Inhibitor Research with Impressive Achievements and New Future Prospects. *J Med Chem* **65**:891–892.

Lu J, Chen M, Qin Y. 2021. Drug-induced cell viability prediction from LINCS-L1000 through WRFEN-XGBoost algorithm. *BMC Bioinformatics* **22**:13.

Lu J, Chen M, Qin Y, Yu X. 2021. [Prediction of drug-induced cell viability by SAE-XGBoost algorithm based on LINCS-L1000 perturbation signal]. *Sheng Wu Gong Cheng Xue Bao* **37**:1346–1359.

Nusinow DP, Szpyt J, Ghandi M, Rose CM, McDonald ER 3rd, Kalocsay M, Jané-Valbuena J, Gelfand E, Schweppe DK, Jedrychowski M, Golji J, Porter DA, Rejtar T, Wang YK, Kryukov GV, Stegmeier F, Erickson BK, Garraway LA, Sellers WR, Gygi SP. 2020. Quantitative Proteomics of the Cancer Cell Line Encyclopedia. *Cell* **180**:387–402.e16.

O'Brien SG, Guilhot F, Larson RA, Gathmann I, Baccarani M, Cervantes F, Cornelissen JJ, Fischer T, Hochhaus A, Hughes T, Lechner K, Nielsen JL, Rousselot P, Reiffers J, Saglio G, Shepherd J, Simonsson B, Gratwohl A, Goldman JM, Kantarjian H, Taylor K, Verhoef G, Bolton AE, Capdeville R, Druker BJ, IRIS Investigators. 2003. Imatinib compared with interferon and low-dose cytarabine for newly diagnosed chronic-phase chronic myeloid leukemia. *N Engl J Med* **348**:994–1004.

Plowright AT, editor. 2019. Target Discovery and Validation: Methods and Strategies for Drug Discovery, Methods and Principles in Medicinal Chemistry. Wiley.

Pottier C, Fresnais M, Gilon M, Jérusalem G, Longuespée R, Sounni NE. 2020. Tyrosine Kinase Inhibitors in Cancer: Breakthrough and Challenges of Targeted Therapy. *Cancers* **12**. doi:10.3390/cancers12030731

Ritz C, Baty F, Streibig JC, Gerhard D. 2015. Dose-Response Analysis Using R. *PLoS One* **10**:e0146021.

Seebacher NA, Stacy AE, Porter GM, Merlot AM. 2019. Clinical development of targeted and immune based anti-cancer therapies. *J Exp Clin Cancer Res* **38**:156.

Shapiro P. 2020. Next Generation Kinase Inhibitors: Moving Beyond the ATP Binding/Catalytic Sites. Springer, Cham.

Slamon DJ, Leyland-Jones B, Shak S, Fuchs H, Paton V, Bajamonde A, Fleming T, Eiermann W, Wolter J, Pegram M, Baselga J, Norton L. 2001. Use of chemotherapy plus a monoclonal antibody against HER2 for metastatic breast cancer that overexpresses HER2. *N Engl J Med* **344**:783–792.

Solomon BJ, Mok T, Kim D-W, Wu Y-L, Nakagawa K, Mekhail T, Felip E, Cappuzzo F, Paolini J, Usari T, Iyer S, Reisman A, Wilner KD, Tursi J, Blackhall F, PROFILE 1014 Investigators. 2014. First-line crizotinib versus chemotherapy in ALK-positive lung cancer. *N Engl J Med* **371**:2167–2177.

Szklarczyk D, Gable AL, Nastou KC, Lyon D, Kirsch R, Pyysalo S, Doncheva NT, Legeay M, Fang T, Bork P, Jensen LJ, von Mering C. 2021. The STRING database in 2021: customizable protein-protein networks, and functional characterization of user-uploaded gene/measurement sets. *Nucleic Acids Res* **49**:D605–D612.

Tsherniak A, Vazquez F, Montgomery PG, Weir BA, Kryukov G, Cowley GS, Gill S, Harrington WF, Pantel S, Krill-Burger JM, Meyers RM, Ali L, Goodale A, Lee Y, Jiang G, Hsiao J, Gerath WFJ, Howell S, Merkel E, Ghandi M, Garraway LA, Root DE, Golub TR, Boehm JS, Hahn WC. 2017. Defining a Cancer Dependency Map. *Cell* **170**:564–576.e16.

Vidović D, Koleti A, Schürer SC. 2014. Large-scale integration of small molecule-induced genome-wide transcriptional responses, Kinome-wide binding affinities and cell-growth inhibition profiles reveal global trends characterizing systems-level drug action. *Front Genet* **5**:342.

Wright MN, Ziegler A. 2017. ranger: A Fast Implementation of Random Forests for High Dimensional Data in C++ and R. *J Stat Softw* **77**:1–17.

Yesilkanal AE, Yang D, Valdespino A, Tiwari P, Sabino AU, Nguyen LC, Lee J, Xie X-H, Sun S, Dann C, Robinson-Mailman L, Steinberg E, Stuhlmiller T, Frankenberger C, Goldsmith E, Johnson GL, Ramos AF, Rosner MR. 2021. Limited inhibition of multiple nodes in a driver network blocks metastasis. *Elife* **10**. doi:10.7554/eLife.59696

Yuan M, Huang L-L, Chen J-H, Wu J, Xu Q. 2019. The emerging treatment landscape of targeted therapy in non-small-cell lung cancer. *Signal Transduct Target Ther* **4**:61.

Yu C, Mannan AM, Yvone GM, Ross KN, Zhang Y-L, Marton MA, Taylor BR, Crenshaw A, Gould JZ, Tamayo P, Weir BA, Tsherniak A, Wong B, Garraway LA, Shamji AF, Palmer MA, Foley MA, Winckler W, Schreiber SL, Kung AL, Golub TR. 2016. High-throughput identification of genotype-specific cancer vulnerabilities in mixtures of barcoded tumor cell lines. *Nat Biotechnol* **34**:419–423.

Zawistowski JS, Bevill SM, Goulet DR, Stuhlmiller TJ, Beltran AS, Olivares-Quintero JF, Singh D, Sciaky N, Parker JS, Rashid NU, Chen X, Duncan JS, Whittle MC, Angus SP, Velarde SH, Golitz BT, He X, Santos C, Darr DB, Gallagher K, Graves LM, Perou CM, Carey LA, Earp HS, Johnson GL. 2017. Enhancer Remodeling during Adaptive Bypass to MEK Inhibition Is Attenuated by Pharmacologic Targeting of the P-TEFb Complex. *Cancer Discov* **7**:302–321.

Zhong L, Li Y, Xiong L, Wang W, Wu M, Yuan T, Yang W, Tian C, Miao Z, Wang T, Yang S. 2021. Small molecules in targeted cancer therapy: advances, challenges, and future perspectives. *Signal Transduct Target Ther* **6**:201.